Master of Science in Materials Engineering for Industry 4.0

Polytechnic University of Turin, Italy

MATERIAL AND DESIGN

PROJECT WORK REPORT ON “TURBINE BLADE”

Siriro, Wiseman, S333263

Submitted to:

Prof. Daniel Ugues
Prof. Paolo Fino
Prof. Mariangela Lombardi
Dr. Leonardo Iannucci
Dr. Alessandra Martucci

20/06/2024

Table of Contents.

1 Introduction on the selected component.

Turbine blade is a critical component of a gas turbine engine which is subjected to high temperature. They are the principal elements that convert heat energy into kinetic energy. Their dimensions and their shape determine overall efficiency, reliability, and lifespan. These blades are subjected to rotational forces, extreme pressures, and high temperature which is generated in the combustion chamber as indicated in figure 1 below.

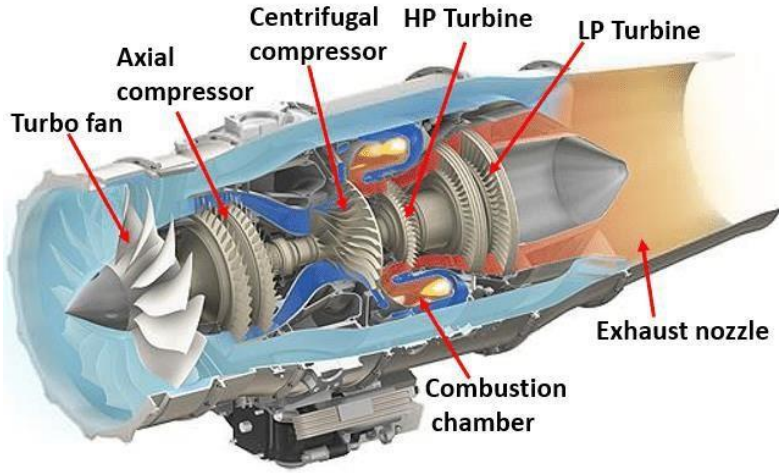

Figure 1. basic components of turbofan gas turbine engine [24]

In the realm of mobility and transportation, gas turbines have emerged as significant and dependable power production technology. Because they have a high power to weight ratio and are lightweight and small, gas turbines are especially well-suited for use in aircraft propulsion. There are three different types of gas turbine engines: turbojet, turbofan, and turboprop [1].

A high-pressure turbine that just drives the compressor often experiences some expansion in a turbine driving an external load, with the remainder expansion occurring in a different, "free" turbine that is connected to the load [2].

The gas turbine has an air inlet, a compressor stage (driven by the high-pressure turbine), a combustion chamber, and high-pressure and low-pressure turbines. The compressed air that passes through the compressor stage mixes with the fuel in the combustion chamber, where it is ignited, and then hot gases flow to drive the main power turbine stages.

The operational principle of gas turbine engine is based on Bryton cycle. The following figure shows the temperature, pressure and flow variation in turbojet engines.

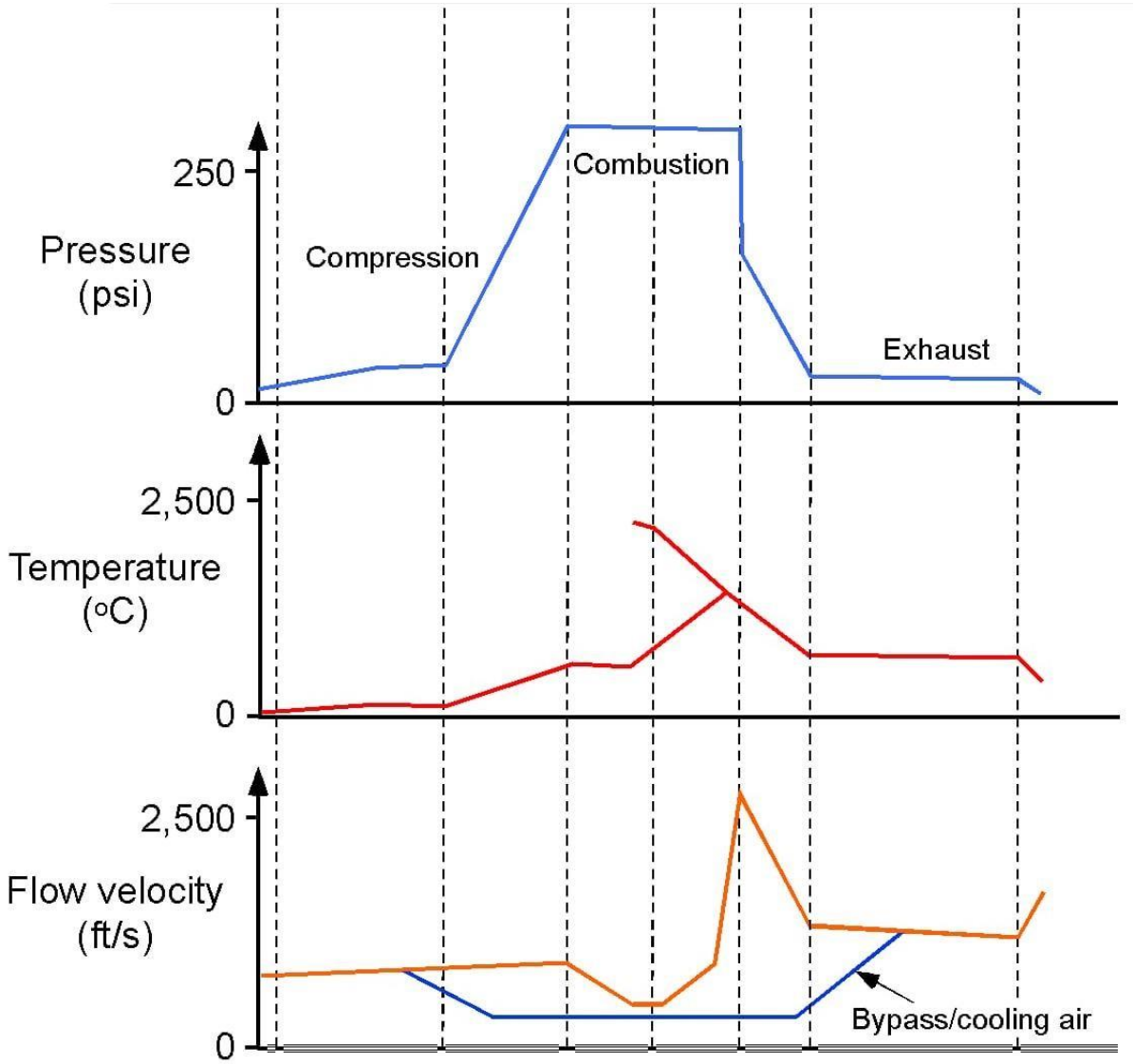

Figure 2. Representative pressure, temperature, and flow velocity variations through a turbojet engine [25]

The airfoil shape of the blade (figure 2) Allows the blade to efficiently extract energy from the hot gases and convert it into rotational motion.

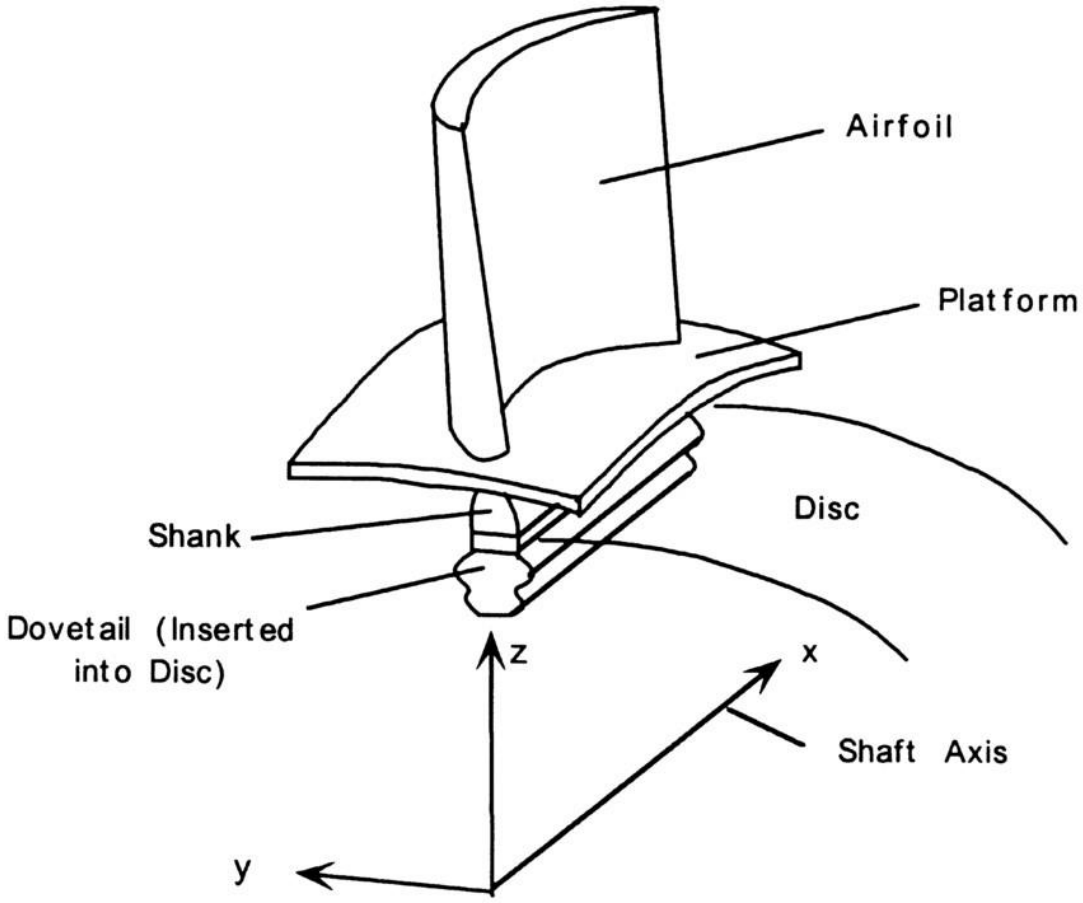

Figure 3. A schematic of a high-pressure turbine blade [26]

Turbine blades in gas turbine engines operate under extremely harsh conditions, including very high temperatures, significant centrifugal forces, and constant vibrations. To ensure the performance and longevity of these blades, selecting the right materials is crucial. This project will perform a comprehensive material selection process for first stage high-pressure turbine blades for domestic commercial aircraft engine using Granta software and other relevant selection criteria. We will carefully assess potential materials using Granta software. For screening resources according to particular needs, Granta software provides an extensive database together with sophisticated capabilities. The process is as follows: first, performance criteria are defined according to operational conditions; then, materials that satisfy basic requirements such as high temperature strength, oxidation resistance, and density are filtered using Granta software; the shortlisted materials are ranked according to their performance in terms of creep resistance, fatigue

resistance, and thermal conductivity; finally, a thorough analysis of the materials that ranked highest is carried out. The mechanical, thermal, and long-term behavior under operating settings will all be examined in this project. Ultimately, the best material will be chosen, and the decision will be supported by a thorough analysis of all pertinent variables.

2 Table function, objectives and constraints.

Table. 1. Table function, objectives and constraints

Fonction	ensure energy transfer between the gas and the rotor
Objective	Maximize creep strength Minimize mass Maximize fracture toughness Maximize fatigue strength
Contraints	Service Temperatures >800°C Coefficient of Thermal Expansion < 12*10-6 /°C Excellent Corrosion Resistance Thermal conductivity between 5 W/m*°C and 50 W/m*°C Youngs Modulus >100GPa

Turbine blades are exposed to loads that can cause failure during operation, therefore, the gas turbine blade component must be designed with consideration the combined effect of centrifugal loading and thermal stresses induced on the blade in service condition [3]. When a material is loaded at a temperature above about one third of its absolute melting point, Tm, it **creeps**. Creep is time dependent deformation phenomenon that plagues material subjected to constant stress at elevated temperatures. Over extended periods, the material elongates or deforms plastically without any increase in applied stress. In design against creep, we seek the material which will carry the design loads without failure, for the design life at the design temperature [4][5].

A turbine blade is subjected to huge centrifugal load, which will be one of our critical factors in selecting the material. The blades also must not fail due to bending during sudden turbine acceleration or vibrations. This requires high strength and resistance to brittle failure. Resistance to fast fracture, which would result in catastrophic failure with blades becoming projectiles, as well as resistance to centrifugal loading. The fracture will be governed by crack initiation and propagation of cracks properties (**Fracture toughness**).

Fatigue failure is one of the most important factors which can cause the damage of the turbine blade.

The high rpm of the turbine also results in stresses induced from the generated centrifugal forces which can result in creep conditions [1]. For the centrifugal forces, we look for high strength in combination with low density for this application. Tensile strength, Yield strength or Fatigue strength are possible mechanical properties to consider. The cyclic load does not refer to the rotations of the turbine, but rather to the load caused by frequent and repetitive starts, stops, thermal shocks etc. We can consider **Fatigue strength**, to withstand many cycles of fluctuating loads or cyclic loading. Low density of material is also used to minimize both the power needed to drive the turbine (improve efficiency) and the total weight of the engine.

To find low weight with high fracture toughness, high fatigue strength and high stiffness material, the Edupack Granta software is used. And the thermal, mechanical and durability constraints are determined through literature survey as follows.

Advanced gas turbine engines' turbine section blades operate in extremely stressful conditions, in high temperatures, and in gas environments that are typically highly oxidizing and frequently contain corrosive fuel residues and ingested salts [6]. To withstand oxidizing and resist corrosion at high temperature the material should be highly corrosion resistant.

Under the investigation [7] the Rolls Royce Turbine, turbine blade operates at high temperature was analyzed thermal stress at 816 °C for cast based nickel alloy IN-738 which melted temperature of between **1230-1315 ºC.** According to Rolls Royce, during the past 70 years, the turbine entry temperature has increased from 1000 K for Whittle engine to higher than 1800 K for Trent 900. The material used in the high-pressure turbine is usually nickel based super alloy should have high service temperature (700°C and above) to withstand the high temperature environment [1]. **Rolls Royce** [8] reported that the 5th stage of the low-pressure and high-pressure turbine operates at a

temperature of about 900°C and 1500°C respectively. For Gas **turbines 9EGE type**, gas temperatures at the turbine inlet between 1200ºC to 1600ºC, but some due to un expectable condition and overloading have boosted inlet temperatures as high as 1600ºC. The precipitation-hardened nickel-base super alloy with good strength, ductility, and fracture toughness material was selected for the part production [9].

Based on the above literature survey, the material to be selected must be withstand high operating temperatures and to be able to withstand tensile and bending stresses and hence should have high value of Young's Modulus. We are interested in service temperatures greater than 800°C which is found around the melting points of superalloys and greater than 100GPa Young's Modulus for effective mechanical properties.

Under the range of service temperature (900 °c) and high speed around (40000 rpm) [3], the ANSYS workbench 2023 R2 demonstrates its effect on SolidWorks model for engine turbine blade material (nickel-based supper alloy) (7) at static structural as shown below.

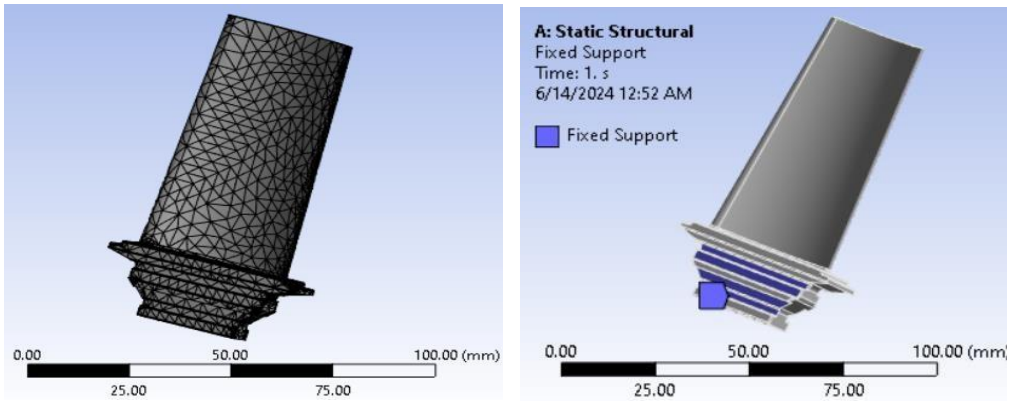

Figure 4. Gas Turbine Blade Meshed Blade and fixed support

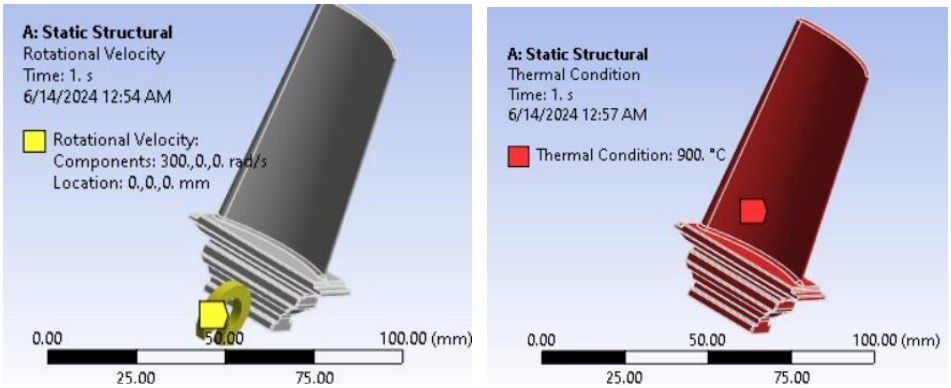

Figure 5. Loading under centrifugal loading (due to rotational speed and b cyclic load due to temperature.

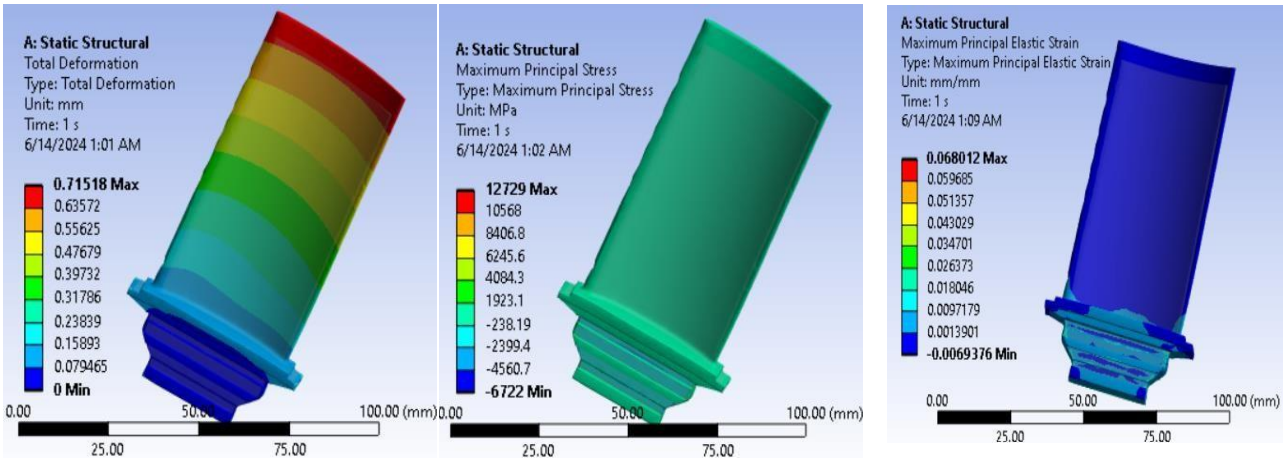

Figure 6. Effects of loading a) total deformation, b) maximum principal stress and c) maximum principal elastic strain

The thermal shock resistance of material which is ability to withstand rapid and significant changes in temperature without cracking or failing are also the determinantal properties to for engine turbine blade. As much as possible high thermal resistance properties material is good for engine turbine blade.

The thermal shock resistance of a material can be quantitatively assessed using the following formula:

$$R = (K * \sigma t) / (\alpha * E * \Delta T)$$ [27]

Where: R is the thermal shock resistance, K represents thermal conductivity, σt is the tensile strength, α is the thermal expansion coefficient, E stands for the elastic modulus, and ΔT is the temperature change.

The above equation relates thermal shock resistance of the material with thermal conductivity and coefficient of thermal expansion. Increasing thermal conductivity increases thermal shock resistance of the material. But very high thermal conductivity may result in reduction of thermal efficiency due to heat dissipation [21] for this reason and most super alloy materials are found in moderate thermal conductivity range from 5 W/m*K to 50W/m*K. Also minimizing Coefficient of thermal expansion improves thermal shock resistance of the material to keep strain and thermal

stresses. We are also interested in the coefficient of thermal expansion less than 12 $*10^{-6}K^{-1}$ for this Granta material selection mini project.

3 Material selection Through Granta

3.1 Application of constraints for Gas Turbine Blade

3.1.1 Application of Thermal Properties as a Constraint.

Since the turbine engines are subjected to harsh environment, it is very important to limit the working conditions to which the materials are exposed thermally. The table below shows the thermal constraints applied for the project and suitable number of materials under this condition. Applying all thermal constraints 157 materials were listed for selection.

Figure 7. Thermal property constraints

3.1.2 Application of mechanical properties as a constraint

To efficiently optimize our objective for this project limiting young's modulus which directly affect stiffness is an essential constraint. In the table below the list of all the materials after applying thermal and mechanical constraints are indicated.

Figure 8. Mechanical property constraint

3.1.3 Application of durability characteristics as a constraint

Regarding the durability features, the component's capacity to withstand exposure to high temperature oxidation must be considered.

Figure 9. Durability constraints

After applying all the constraints of thermal, mechanical and durability properties total 126 materials of different families are proposed by Granta Edu pack. The figure below indicates the diagram of youngs modulus against density for all proposed materials.

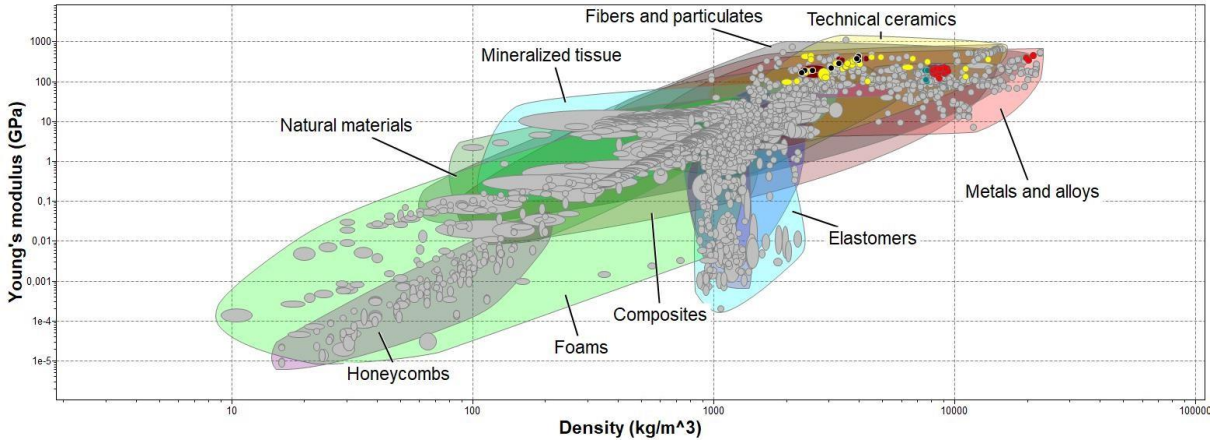

Figure 10. Youngs modulus Vs Density

3.2 Application of Performance Index

The screening and ranking process links design technical and economic requirements to database attributes, based on material properties that represent component performance. Material performance indices help quantify how well a material performs for a specific design. They consider both the material properties and the design requirements (function, geometry) to identify

the best material for the job [10][11]. This simplifies material selection, especially in the early design stages. Material performance is described by an equation (1) that considers function (F), geometry (G), and material properties (M).

$$P = f(F, G, M) \quad (1)$$

The performance of a component, such as its mass, volume, cost, or life, is expressed by the performance metric, P. Depending on the functional needs, the ideal design entails choosing materials and shape to maximize or minimize P. The performance index is the product of three functions, f1, f2, and f3, provided the parameters are independent [10][11]. Following that, the performance index is determined as

$$P = f1\,(F)\square\, f2\,(G)\square\, f3\,(M) \quad (2)$$

A simplified version (2) separates these factors into a product of functions:

- f1(F) x f2(G) - structural efficiency coefficient (combines function and geometry)
- f3(M) - material efficiency coefficient

This allows focusing on minimizing the material factor (f3(M)) to find the best material without solving the entire design problem at once. This simplification allows choosing a material that minimizes f3(M) for optimal performance without solving the entire design problem upfront. Material performance indices can be customized (Mp = f3(M)) for specific design needs (stiffness, strength, etc.) on various structural components (beams, columns). This simplifies material selection for different design goals.

For turbine engine turbine blade, the following two main assumptions have been made in for determining the performance indices or to obtain specific applicable material.

a. The blade is a cantilever fixed at one end and uniformly loaded as shown in Figure 4.

b. The cross-sectional area of the blade is a free variable with a constant aspect ratio α

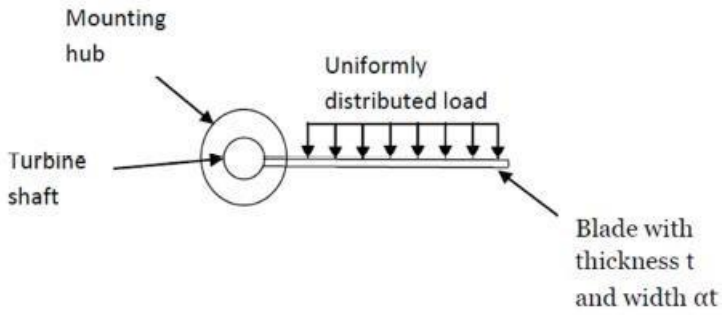

Figure 11. Engine Turbine blade as a cantilever with uniform loading [8]

To improve the service life, efficiency and to perform its function properly, of the engine turbine performance index should minimize mass, maximize fracture toughness and maximize fatigue strength under thermal, mechanical and durability characterize constraints. Since Granta are not supported to investigate creep time dependent behavior.

3.2.1 Application of bending strength to minimize mass.

From the generic beam bending equation

$$\frac{M}{I} = \frac{\sigma}{y} \tag{3}$$

Where:

σ is the stress at distance y from neutral axis of beam; M is the bending moment of the blade; y is the distance from the neutral axis; and I is the second moment of area. For a uniformly distributed load on a cantilever,

$$M = \frac{wl^2}{2} \tag{4}$$

Where: w is the uniformly distributed load in N/m; l is the length of the blade in meter.

$$I = \frac{\alpha t^4}{12} \tag{5}$$

Where

t is the thickness of blades; α is the aspect ratio. For stress $(\sigma) = \sigma_{\max}$

$$t$$

$$y = \frac{}{2} \tag{6}$$

From equation 6

$$\frac{I}{y} = \frac{[\alpha t^4]}{\frac{1}{[2]}} = \frac{\alpha t^3}{6} \tag{7}$$

$$= \frac{}{6}\left(\sqrt{\frac{A}{\alpha}}\right)^{3} = \frac{A^{\frac{3}{2}}}{6\sqrt{\alpha}}$$

Cross sectional Area,

$$A = \alpha t^2 \tag{8}$$

Substituting the value of t from equation 7 into 8 gives

$$\frac{I}{y} \quad \alpha \tag{9}$$

From equation 1,

$$\frac{}{\text{max}} = \frac{}{2\sigma_{\text{max}}} = \frac{\frac{3}{2}}{6\sqrt{\alpha}} \qquad M \quad wl^2 \quad A \tag{10}$$

$$\sigma \qquad \sigma_{\text{max}}$$

Mass of the blade, m_1 is given by

$$m_1 = Al\rho \tag{12}$$

Where: A is the cross-sectional area, and ρ is the material density

Substituting equation 9 into 10,

$$A \tag{11}$$

$$= \left(\frac{3\alpha^{\frac{1}{2}} wl^2}{}\right)^{\frac{2}{3}}$$

$$m_1 = \left(\frac{3\alpha \frac{1}{2} w l^2}{\sigma_{max}}\right)^{\frac{2}{3}} l\rho \quad (13)$$

For $\sigma_{max} = \sigma_y$ (yield strength)

$$m_1 = (3\alpha_2 w l_2)^{\frac{2}{3}} \, l^{\frac{2}{3}} \frac{\rho}{(\sigma_y)^{\frac{2}{3}}} \quad (14)$$

Taking log on both sides of equation (14)

$$log\,(m1) = log(\rho) - 2/3log\,(\sigma_y)$$

$$log(\rho) = 2/3log\,(\sigma_y) + (log\,(m1)) \quad (15)$$

Therefore, to minimize mass, the material index $\left(\frac{\sigma_y}{\rho}\right)^{\frac{2}{3}}$ should be maximized.

To optimize mass by applying the performance index derived above for bending strength, the diagram of yield strength Vs density is plotted

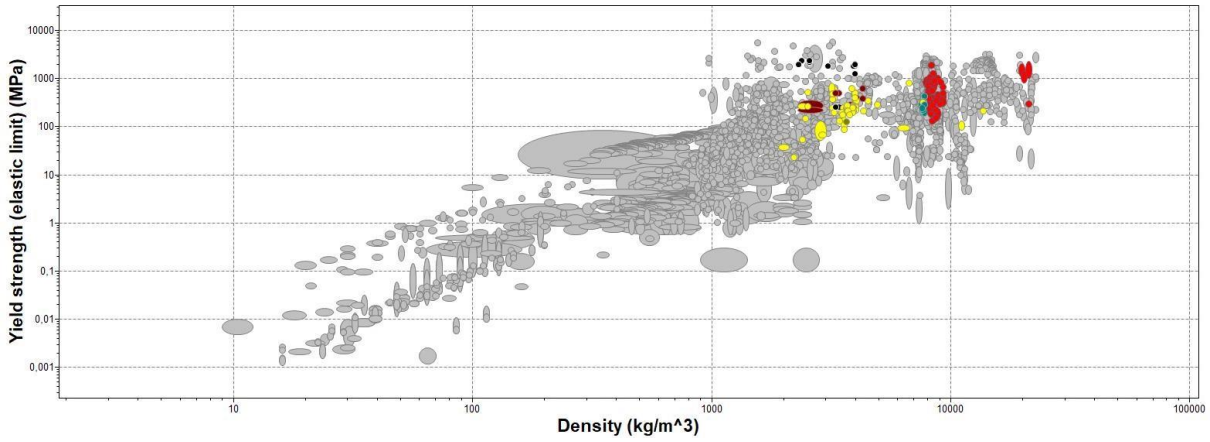

Figure 12. yield strength Vs density

Then by applying the material index line calculated above which has a slope of 0.667, to optimize the mass, materials below the line are eliminated as indicated in the figure below.

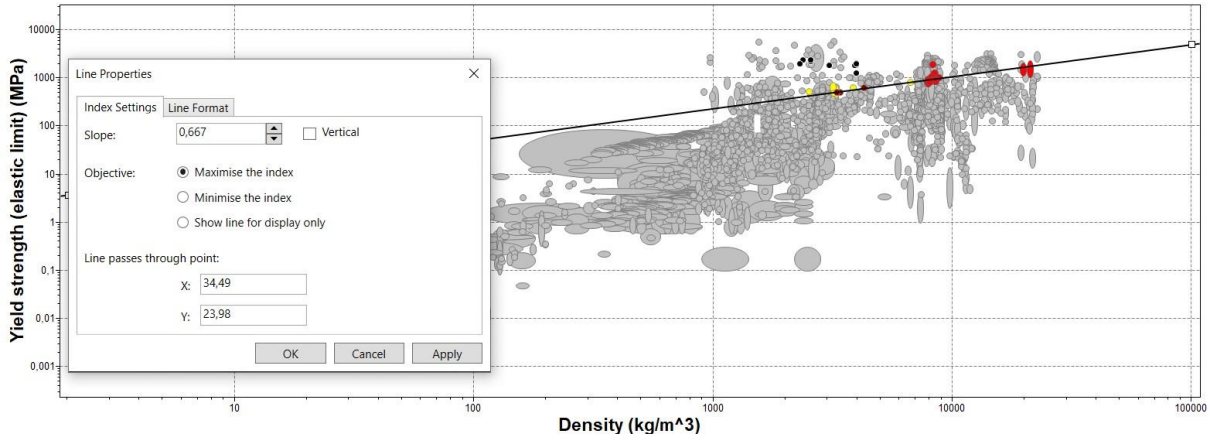

Figure 13. yield strength Vs Density after applying index line

3.2.2 Application of Material stiffness property to minimize mass

The stiffness of a beam is given by Ashby [10][8][12].

$$S = \frac{F}{\Delta} \tag{16}$$

Where: S is the stiffness of the material, F is the load applied, Δ is the deflection. In this case,

$$S = \frac{wl}{\left(\frac{wl}{8EI}\right)} \frac{8EI}{l^3} = l^2 \tag{17}$$

Where E is the Young's Modulus of the material Substituting equation 5 into 28

$$S = \frac{8E\alpha t^4}{12l^2} \tag{18}$$

$$t = \left(\frac{12Sl^2}{8E\alpha}\right)^{\frac{1}{4}} \tag{19}$$

$$m_4 = Alp = \alpha t^2 l\rho \tag{20}$$

Substituting equation 19 into 20,

$$m^4 = \alpha\left(\frac{12Sl^2}{8E\alpha}\right)^{\frac{1}{2}} l\rho$$

$$m_4 = \sqrt{\alpha}\left(\frac{12S}{8}\right)^{\frac{1}{2}} l\left(\frac{\rho}{\bar{E}_2}\right) \quad (21)$$

Taking log on both sides of equation (14)

$$log\ (m4) = log(\rho) - 1/2 log\ (E)$$

$$log(\rho) = 1/2\ log\ (E) + (log\ (m4) \quad (22)$$

In order to optimize performance indices $m_4 = m_1$. Therefore, to minimize mass, $\frac{E^{\frac{1}{2}}}{\rho}$ should be maximized.

Then the following diagram is plotted for the optimization of stiffness.

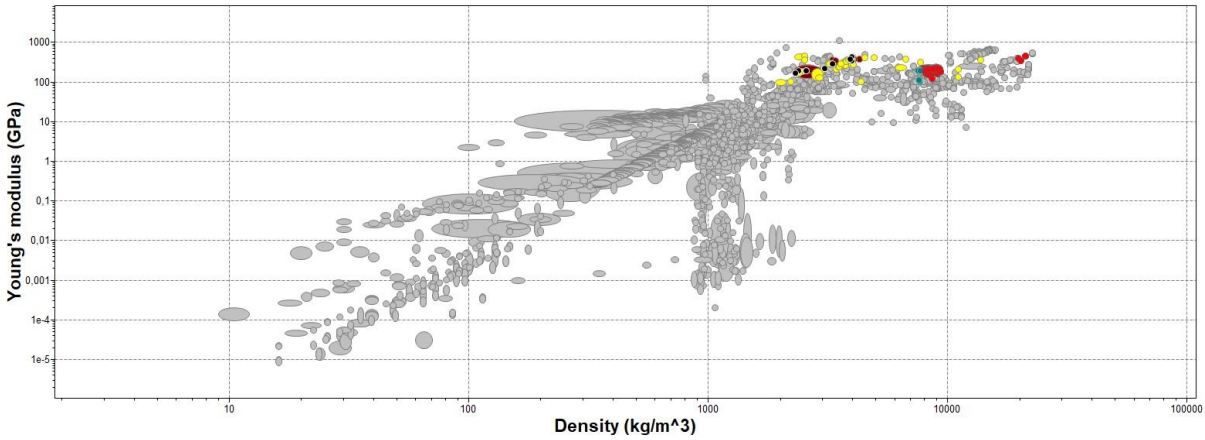

Figure 14. Youngs modulus Vs Density

Then by applying the material index line which we drive in equation (21) above which has a slope of 0.5, to optimize the index, materials below the line are eliminated as indicated in the figure below.

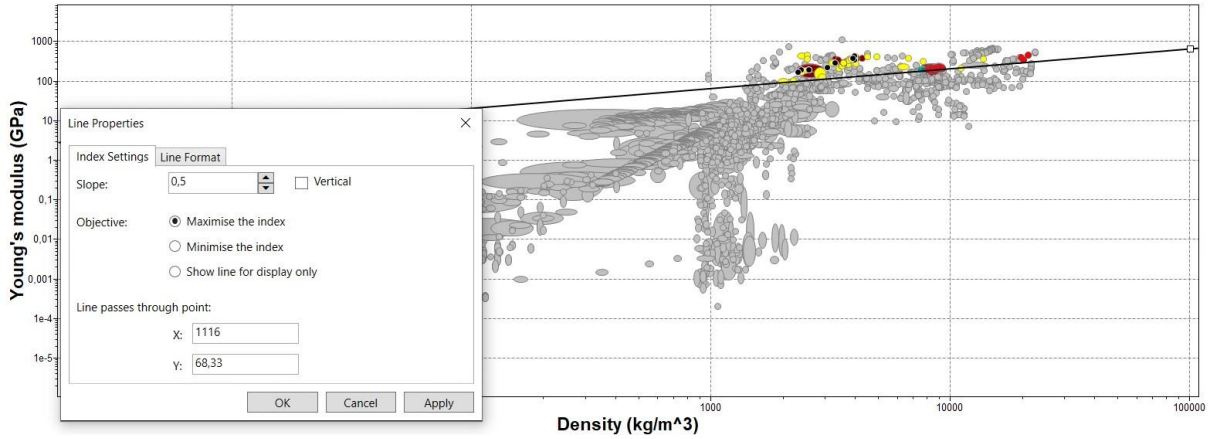

Figure 15. Youngs modulus Vs density diagram after applying index line

3.2.3 Application of Performance Index to maximize Fatigue strength

It is desired that the Fatigue strength endurance limit σ_e be as high as possible [10][8][12]. Hence,

$$\frac{wl}{A} \leq \sigma_e \tag{23}$$

Where wl is the total load on the blade,

$$A \geq \frac{wl}{\sigma_e} \tag{24}$$

Mass, $m_2 = Al\rho$

$$m_2 = wl \frac{\rho^2}{\sigma_e} \tag{25}$$

Taking log on both sides of equation (25)

$$log\ (m2) = log(\rho) - log\ (\sigma_e)$$

$$log(\rho) = log\ (\sigma_e) + (log\ (m2)) \tag{26}$$

In order to optimize performance indices $m_2 = m_1$. To minimize mass, $\frac{\sigma_e}{\rho}$ should be maximized

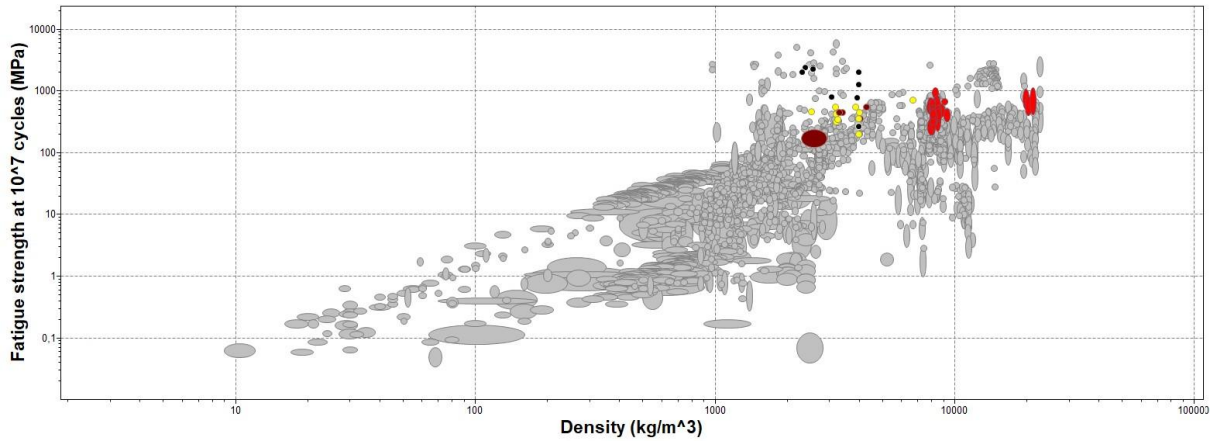

Figure 16. Fatigue strength Vs density

Then by applying the material index line calculated above which has a slope of 1, to maximize the Fatigue strength, materials below the line are eliminated as indicated in the figure below.

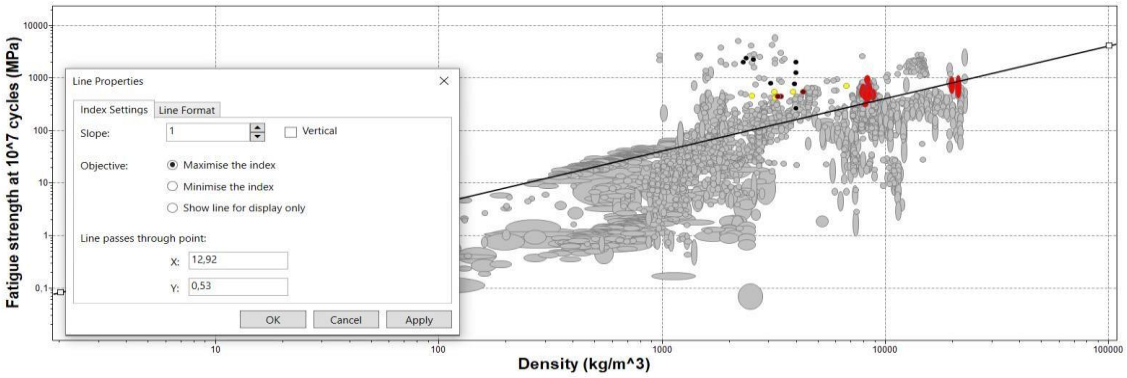

Figure 17. Fatigue strength Vs density after applying index line

3.2.4 Application of Performance Index to Maximize Fracture Toughness

Assuming that the blade follows the equation of a center cracked plate with a very large width [8][9][10].

$$K_{1c} = \sigma(\pi c)^{0.5} \text{ Where:} \quad (27)$$

K1c is the fracture toughness, σ is the applied stress and, c is a very small crack.

$$K_{1c} = \frac{wl}{A}(\pi c)^{0.5} \quad (28)$$

$$= wl\,(\pi c)^{0.5} \quad (20)$$

$$\frac{A}{K_{1c}}$$

$$m_3 = Al\rho \quad (30)$$

$$m_3 = \left(\frac{wl}{K_{1c}}\right)^{0.5} \quad (32)$$

$$m_3 = wl^2(\pi c)^{0.5}\left(\frac{\rho}{K_{1c}}\right)$$

Taking log on both sides of equation (32)

$$log\,(m3) = log(\rho) - log\,(K_{1c})$$

$$m = \frac{}{}(\pi c)\quad l\rho \quad (31)$$

$$log(\rho) = log\,(K_{1c}) + (log\,(m3) \quad (33)$$

In order to optimize performance indices $m_3 = m_1$ To minimize mass, $\frac{K_{1c}}{\rho}$ should be maximized.

The figure below shows the graph of fracture toughness Vs density plotted to apply the index line to optimize our objective of maximizing fracture toughness.

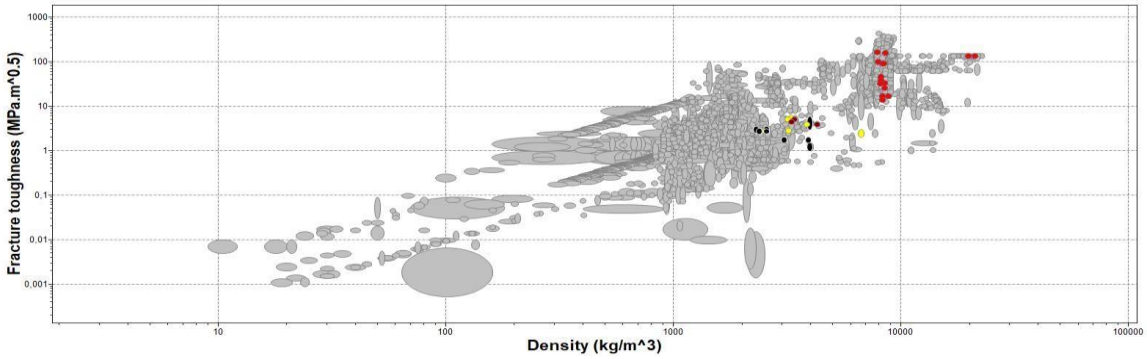

Figure 18. Fracture toughness Vs density

Materials below the line are then excluded as shown in the figure below in order to maximize the fracture toughness by applying the material index line obtained above, which has a slope of 1.

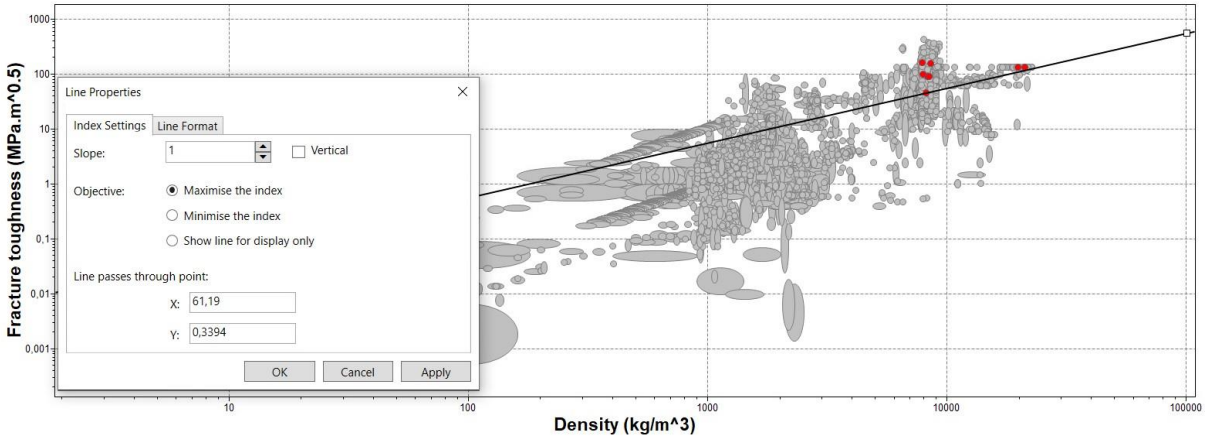

Figure 19. Fracture toughness Vs Density after applying performance index

After applying all the constraints and performance index for each objective on Granta Software, we have found 8 candidate materials as shown in the figure below.

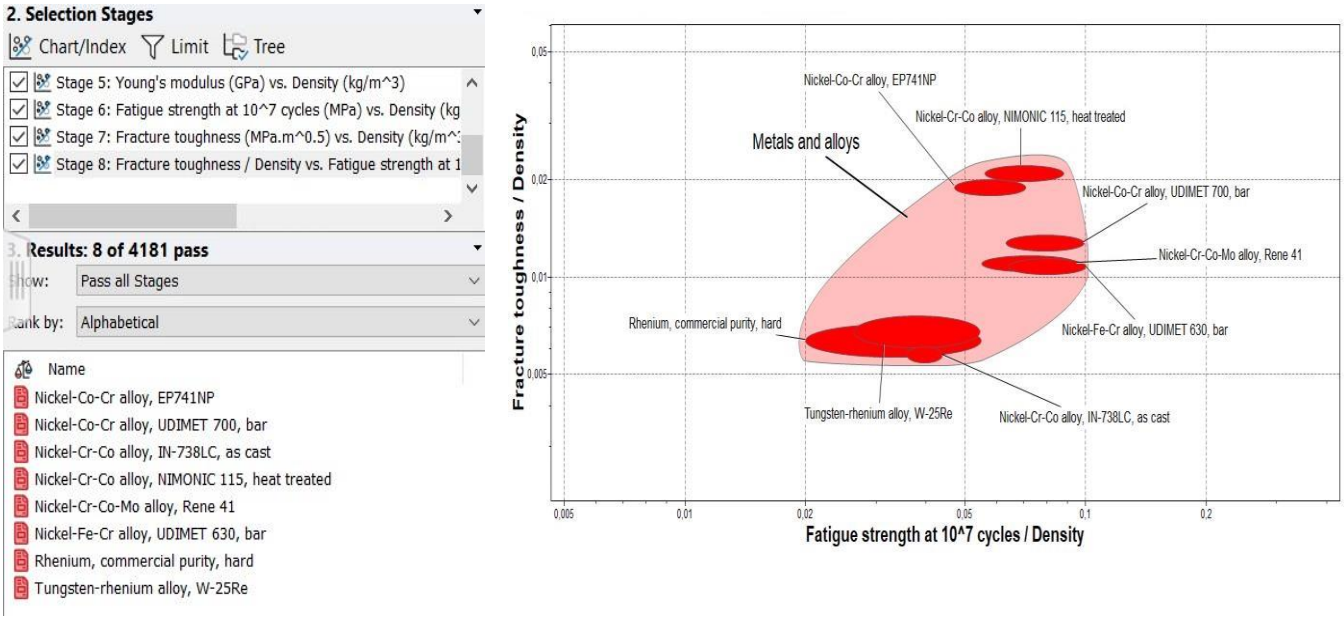

Figure 20. Candidate materials for final selection

Turbine blade casting is a critical process in the manufacture of turbine blades for sustainable and batch production. Turbine blades are complex shapes that must be able to withstand extreme temperatures and stresses, complex shapes with good dimensional accuracy. There are several different casting processes that can be used to manufacture turbine blades, but the most common is investment casting, also known as lost-wax casting. Molten metal, typically a nickel-based superalloy, is then poured into the mold. The application area and manufacturing method for the all-candidate material are investigated on Granta software database. Among 8 candidate material, Nickel -Cr-Co alloy IN-738LC is castable and commonly applicable in turbine blade material as shown figure below.

General information

Designation

Nickel-Cr-Co alloy, IN-738LC, as cast

Condition	As cast

Tradenames

MSRR 7168, 7173, Rolls Royce (UK)
B50A563B, GE (USA)
LA155, Turbomeca (FRANCE)
EMS 55445, Garrett (USA)
SUPERMET 738LC, Firth Rixson (USA)

Typical uses

Industrial gas turbines and jet engine components, e.g. blades, vanes, integral-wheels.

Figure 21. Application area of Nickel -Cr-Co alloy IN-738LC (Extracted from Granta data base)

3.2.5 Creep strength and analysis

Determining the best material for creep strength (resistance to creep rupture depending on loading time) is also another object for our turbine blade material selection through Granta. Granta software does not support important time and temperature dependent parameters such as creep strain (Strain vs time graph), Fracture at elevated temperature (creep strain vs exposure time graph) and Stress rupture data (stress Vs time graph). These time dependent parameters are required to estimate the life of the turbine blade. It is difficult to find this important creep behavior on the Granta Software.

Even though Granta does not support creep time and temperature dependent behavior, it is important to investigate creep behavior of the selected material through literature. **Inconel 738LC** has an exceptional creep resistance property due to the formation of fine, dispersed particles called gamma prime (γ') precipitates within the microstructure during heat treatment. This precipitate acts as an obstacle to dislocations in the materials crystal lattice, hindering movement and preventing creep deformations [13][14].

Creep analysis should be performed using the thermomechanical stress level value obtained for the blade air foil, creep life prediction model such as Norton-Bailey, Dorn-Bailey and Larson-Miller Parameter should be considered and compared for the best prediction of life. But it is

difficult to develop model with outperforming experimental tests at a given temperature with time variation.

Through investigation [15], creep analysis was performed for three model for **Inconel 738LC.** Analyzing the creep life prediction results presented using the Norton-Bailey, Dorn-Bailey and Larson-Miller models are 30790hr, 53170 h and 94350 (at 20000 hr) respectively. Among these model Norton-Bailey model estimates an approximate real blade time of 24000 hours determined by blade cracks on the cooling hole.

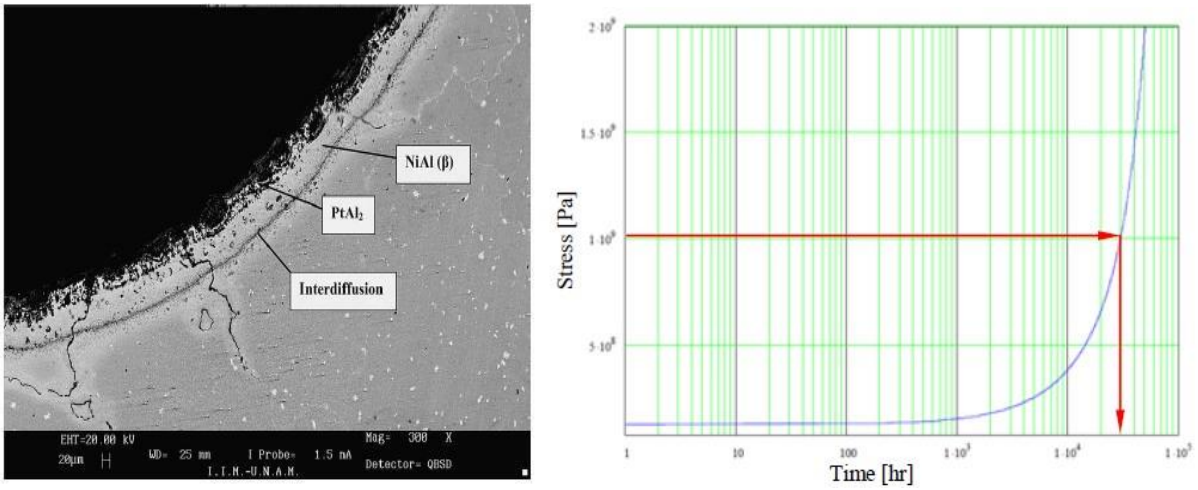

Figure 22. a). Cracks in the central cooling holes and b). Stress variation in the blade for the Norton-Bailey creep model [15].

3.3 General information and Properties of selected material - Nickel Cr-Co-alloy, IN-738LC, as cast

Composition overview

Compositional summary

Ni61-63 / Cr16 / Co8.5 / Al3.2-3.7 / Ti2.4-3.4 / W2.6 / Mo1.8 / Ta1.8 / Nb0.9 / C0.11 / Zr0.03-0.08 / B0.005-0.015 (impurities: Si<0.3, Mn<0.2)

Material family	Metal (non-ferrous)			
Base material	Ni (Nickel)			

Composition detail (metals, ceramics and glasses)

Al (aluminum)	3			%
C (carbon)	0,11			%
Co (cobalt)	8,5			%
Cr (chromium)	16			%
Mo (molybdenum)	1,75			%
Nb (niobium)	0,9			%
Ni (nickel)	61,1	-	61,6	%
Si (silicon)	0	-	0,3	%
Ta (tantalum)	1,75			%
Ti (titanium)	3,4			%
W (tungsten)	2,6			%
Other	0	-	0,2	%

Figure 23. Compositional overview of selected material

Mechanical properties

Young's modulus	195	-	205	GPa
Specific stiffness	24	-	25,4	MN.m/kg
Yield strength (elastic limit)	805	-	990	MPa
Tensile strength	925	-	1,14e3	MPa
Specific strength	99,3	-	122	kN.m/kg
Elongation	5	-	9	% strain
Compressive strength	* 805	-	990	MPa
Flexural modulus	* 195	-	205	GPa
Flexural strength (modulus of rupture)	* 805	-	990	MPa
Shear modulus	74	-	82	GPa
Bulk modulus	140	-	164	GPa
Poisson's ratio	0,27	-	0,29	
Shape factor	18			
Hardness - Vickers	* 350	-	450	HV
Elastic stored energy (springs)	1,63e3	-	2,43e3	kJ/m^3

Fatigue strength model (stress amplitude) 257 - 400 MPa

Parameters: Stress Ratio = -1, Number of Cycles = 1e7cycles

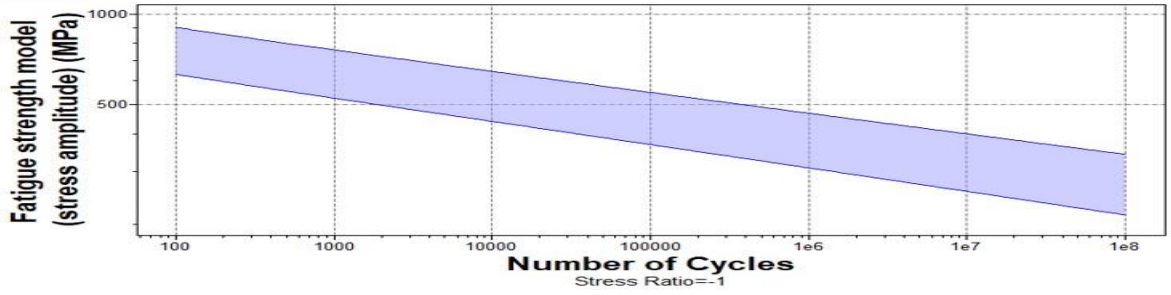

Figure 24. Mechanical properties of selected material

4 Sustainability

Product materials have environmental impacts throughout their life cycle, from extraction to manufacturing. These impacts are primarily due to energy needs, resource usage, and waste production. During the use life cycle, the product requires energy, spare parts, maintenance, and other resources. In the end-of-life phase, the product may be worn out, broken, unfashionable, or dirty, and waste is managed [16]. Designers can assess potential environmental impacts through software during product development, and conscious material choices can help reduce these impacts [16][17].

4.1 Life cycle analysis, challenges. and the Eco Audit tool

Environmental life cycle assessment (LCA) is a method used to evaluate a product's environmental impact, analyzing its post-service life and influencing energy and emissions flows. It is documented in ISO 14040, 1997, and 1998 standards. The Life Cycle Assessment (LCA) method, as per ISO 14040:2006, involves four steps: goal and scope definition, inventory analysis, impact assessment, and interpretation [17][18]. The scope varies depending on the study's goal. Inventory analysis collects data for the study's goals, while impact assessment provides additional information for understanding environmental significance. Interpretation summarizes impact assessment results for conclusions, recommendations, and decision-making, considering completeness, sensitivity, and consistency checks. LCA provides crucial information on materials' contribution to environmental impacts, such as ozone depletion, global warming, soil and water acidification, and human toxicity [17][18].

However, LCA methods are subject to uncertainty due to the need for sophisticated monitoring equipment and detailed information. Full LCA can be time-consuming and resource-intensive, making it unsuitable for quick decision-making in early design stages. Designers struggle to balance CO2 and SO_X productions against resource depletion, energy consumption, global warming potential, and human toxicity [17][18].

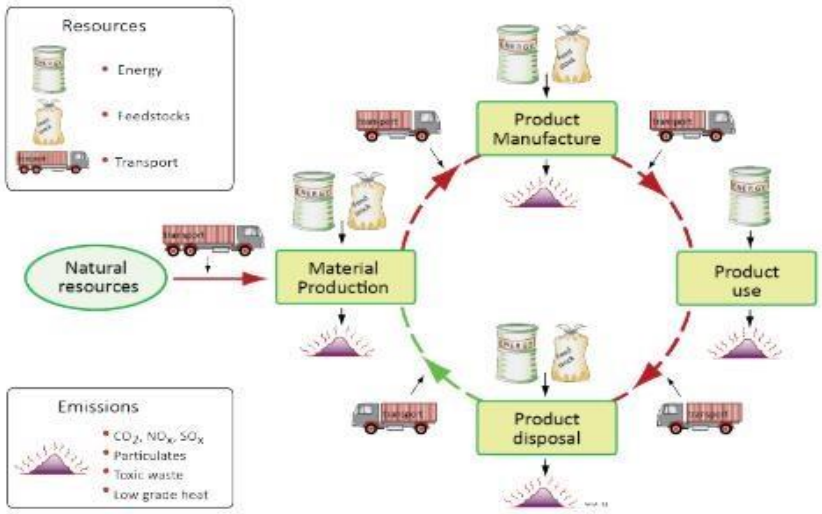

Figure 25. Material Life Cycle [10]

Designers sought a faster, streamlined method to evaluate environmental impact during early design phases. Ansys Granta's material property databases offered an efficient approach. Eco Audit emerged as a solution, simplifying LCA by focusing on key impact areas and utilizing existing data, enabling quicker assessments and targeted decision-making in early design stages [18]. Ashby's "eco-audit" approach is utilized with Ansys Granta software to conduct a carbon footprint study on the selected materials. The tool evaluates a product's environmental impact throughout its entire life cycle, considering six key factors: material, manufacture, transportation, use, disposal, and end-of-life potential. Emission factors were calculated by multiplying them by the average amount of materials collected for each functional unit. The impacts are measured in terms of environmental stressors of energy use [MJ] and CO_2 footprint [kg] [17][18].

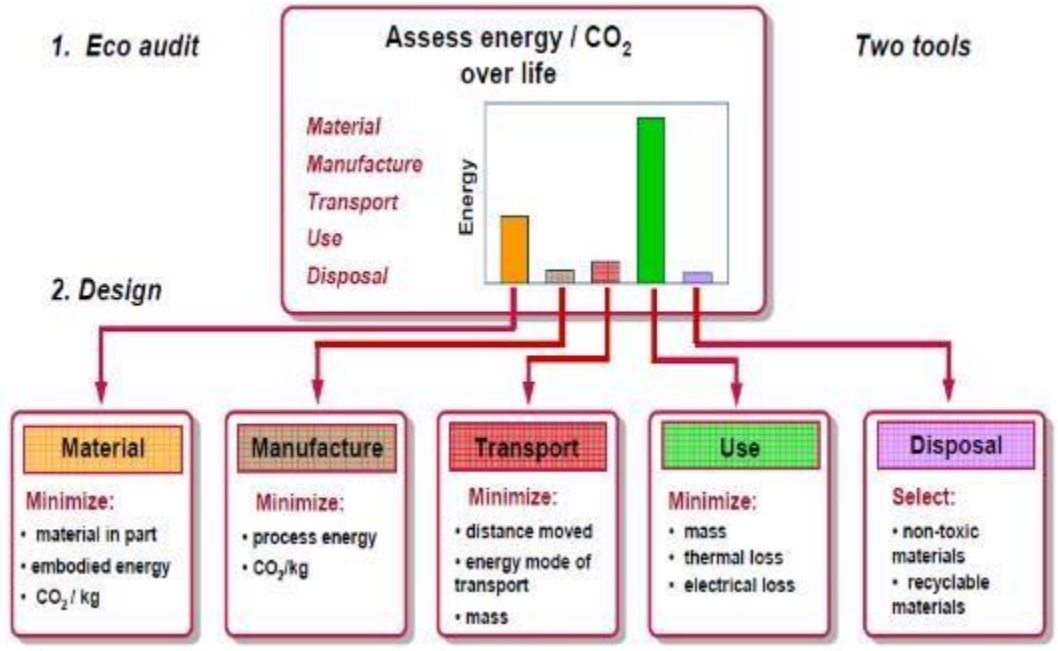

Figure 26. Eco Audit and Strategy for Guiding Eco Design [19]

When manufacturing is a significant energy-consuming phase of life, minimizing processing energy becomes a top priority. When transportation plays a significant role, finding more efficient modes or minimizing distance becomes a top goal. The primary focus in eco design is to reduce processing energies in manufacturing, focusing on efficient transport or reducing distance. When the use phase dominates, strategies include minimizing mass, increasing thermal efficiency, or reducing electrical losses [17]. The best material choice to minimize one phase will not necessarily minimize the others. Rational approaches to eco design involve analyzing the phase of life, guiding redesign and materials selection to minimize environmental impact, and using trade-off methods to guide the choice [18].

The tool's structure consists of two inputs: a user-entered bill of materials, process choice, transport requirements, duty cycle, and disposal route, and data for embodied energies and process energies from a material properties database. The outputs are the energy or carbon footprint of each phase of life, presented as bar charts and tabular form [16][18].

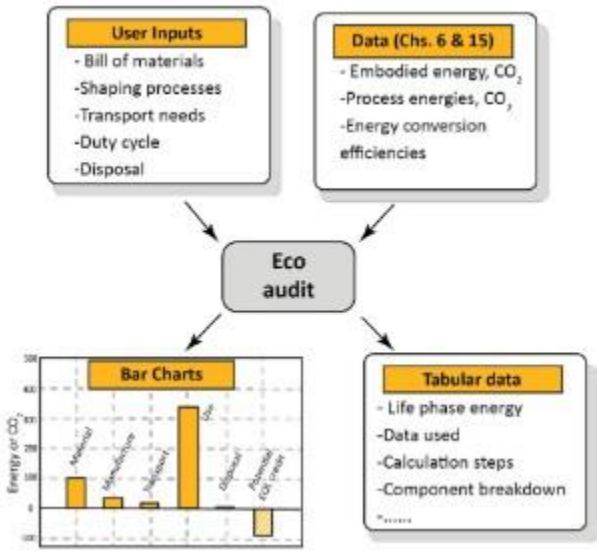

Figure 27. Energy Eco Audit Models [19]

To conduct an eco-audit, we require the bill of materials, manufacturing process, transportation of product parts, duty cycle during usage, and eco data on energy and CO_2 footprints [17]. The material meeting all the objectives and satisfying all the constraints for the aircraft turbine is found in INCONEL 738LC, a nickel-chromium alloy. Ansys Granta was used to assess the sustainability of the material. Initially, the stored information about the material was accessed from the Ansys Granata database. First, general information about the material was accessed, like the designation, use, and composition.

4.2 Data derived using Ansys Granat Database

Various information about Nickel -Cr-Co-alloy, , as cast stored in database acquired as given below in the sub-sections.

4.2.1 Criticality of IN-738LC

According to the study on the critical raw materials for the European Union 2023 [20] Nickel, Aluminum and Titanium, Cobalt, Niobium, Molybdenum, Tungsten, Tantalum are considered to be critical elements. Chemical elements that are considered critical are those that, despite being in high demand, will only be available in limited quantities in the near future [20]. Because IN-738LC contains more than 5% weight of key elements, especially nickel, it exhibits a critical material risk as shown figure below.

Critical materials risk	
Contains >5wt% critical elements?	Yes
Abundance risk level	Medium
Highest risk elements	Niobium, Tungsten, Nickel, Cobalt, Molybdenum, Tantalum
Sourcing and geopolitical risk level	Very high
Highest risk elements	Niobium
Environmental country risk level	High
Highest risk elements	Carbon, Tungsten
Price volatility risk level	Medium
Highest risk elements	Niobium
Conflict material risk level	High
Highest risk elements	Niobium, Tungsten, Tantalum

Figure 28. Critical Material Risk

The information regarding price, physical properties and mechanical properties are given below.

4.2.2 Price, Physical properties and mechanical properties of IN-738LC

Price				
Price	* 27,1	-	32,6	EUR/kg
Price per unit volume	* 2,16e5	-	2,67e5	EUR/m^3
Physical properties				
Density	8e3	-	8,2e3	kg/m^3
Mechanical properties				
Young's modulus	195	-	205	GPa
Specific stiffness	24	-	25,4	MN.m/kg
Yield strength (elastic limit)	805	-	990	MPa
Tensile strength	925	-	1,14e3	MPa
Specific strength	99,3	-	122	kN.m/kg
Elongation	5	-	9	% strain
Compressive strength	* 805	-	990	MPa
Flexural modulus	* 195	-	205	GPa
Flexural strength (modulus of rupture)	* 805	-	990	MPa
Fatigue strength at 10^7 cycles	290	-	355	MPa
Fatigue strength model (stress amplitude)	257	-	400	MPa

Figure 29. Price, Physical properties and mechanical properties of IN-738LC

4.2.3 Processing Properties of IN-738LC

IN-738LC demonstrated suitability for casting. However, Inconel 738 suffers from poor weldability due to its high Ti and Al contents, which leads to solidification cracking and heat affected zone issues [21].

Processing properties	
Metal casting	Acceptable
Metal cold forming	Unsuitable
Metal hot forming	Unsuitable
Weldability	Poor
Notes	Preheating and post weld heat treatments may be required

Figure 30. Processing Properties of IN-738LC

4.3 Typical record showing eco-properties of IN-738LC

4.3.1 Geo-economic data for principal component

Annual world production is the mass of material extracted annually from ores or feedstock, while reserves are estimates of economically recoverable ores or feedstock. These reserves and resource base allow estimates of resource life by dividing them by annual world production, allowing for the time to exhaust resources. The annual production rate for nickel, the principal component of nickel, is around 199 x 10^6 tonne/yr, and the reserve is 74 x 10^6 tonne/yr. Nickel being one of the critical elements in European Union is likely to be imported from high nickel producing countries like Australia, Brazil, Canada China and some other countries listed in the figure below

Geo-economic data for principal component				
Principal component	Nickel			
Typical exploited ore grade	0,997	-	1,1	%
Minimum economic ore grade	0,1	-	2	%
Abundance in Earth's crust	59			ppm
Data note	Minimum value			
Abundance in seawater	5e-4	-	0,002	ppm
Annual world production, principal component	1,99e6			tonne/yr
Reserves, principal component	7,4e7			tonne

Main mining or production areas (metric tonnes per year)

Australia, 240e3
Brazil, 149e3
Canada, 225e3
China, 95e3
Colombia, 75e3
Cuba, 66e3
Dominican Republic, 12.5e3
Indonesia, 440e3
Madagascar, 26e3
New Caledonia, 145e3
the Philippines, 440e3
Russia, 250e3
South Africa, 48e3
Other countries, 274e3

Figure 31. Geo-economic data for principal component of IN-738LC

4.3.2 Primary production of energy, CO2 and water

Fossil fuels like gas, oil, coal, and coke are the primary sources of energy in product life, with some consumed in their current form and most converted to electricity. As for our application, kerosene oil is used in aircraft engines. The embodied energy of a material is the fossil fuel energy

consumed to make one kilogram of material, with some stored in the material for reuse at the end of its life[17][19]. The embodied energy, primary production (virgin grade) ranges from 495-546 MJ/Kg.

The production of 1 kg of material leads to undesired gas emissions, including CO2, NOx, SOx, and CH4, which contribute to global warming, acidification, and ozone-layer depletion [19]. CO2 footprint for primary production (virgin grade) ranges from 24.4.5-26.7 kg/kg

Primary production energy, CO2 and water				
Embodied energy, primary production (virgin grade)	* 495	-	546	MJ/kg
Embodied energy, primary production (typical grade)	* 275	-	326	MJ/kg
CO2 footprint, primary production (virgin grade)	* 24,2	-	26,7	kg/kg
CO2 footprint, primary production (typical grade)	* 14,2	-	16,7	kg/kg
Water usage	* 315	-	349	l/kg

Figure 32. Primary production of energy, CO2 and water

4.3.3 Processing energy, CO2 footprint and water

While IN-738LC is castable as indicated in the above section. The processing of 1 kg of material by using the casting method ranges from 10.1 to 11.1 MJ/kg, while its corresponding CO2 footprint ranges from 0,754 to 0.833 kg/kg.

Processing energy, CO2 footprint & water				
Casting energy	* 10,1	-	11,1	MJ/kg
Casting CO2	* 0,754	-	0,833	kg/kg
Casting water	* 19	-	28,5	l/kg
Vaporization energy	* 1,19e4	-	1,32e4	MJ/kg

Figure 33. Processing energy, CO2 footprint and water

4.3.4 Recycling and End of Life

IN-738LC demonstrated the viability of recycling. Most materials require virgin input to prevent impurities build-up, so the fraction of production that can re-enter the cycle depends on the material and the incorporated product [17]. The fraction of material production that is recycled as a fraction of current supply ranges from 44.7% to 49.4%, as shown in the figure below. While the studies regarding the recyclability of nickel-based alloys rich in chromium for aerospace applications are still in the research phase [22], we consider a recyclability of 30% for our studies.

Recycling and end of life				
Recycle	✓			
Embodied energy, recycling	* 48,7	-	53,8	MJ/kg
CO2 footprint, recycling	* 3,82	-	4,22	kg/kg
Recycle fraction in current supply	44,7	-	49,4	%
Downcycle	✓			
Combust for energy recovery	✗			
Landfill	✗			
Biodegrade	✗			

Figure 34. Recycling and End of Life

4.3.5 Bio-Data

Data bases indicate that nickel is a potentially hazardous material that should be disposed of carefully. Nickel compounds pose a health risk due to their ability to disrupt cellular processes, potentially leading to cancer and fetal abnormalities [23]. Research shows that nickel can damage DNA, interfere with hormones crucial for fetal development, and harm developing organs and tissues, including birth defects [23]

Notes

Warning

All nickel compounds should be regarded as toxic. Some can cause cancer and/or fetal abnormalities.

Figure 35. Bio-data of IN-738LC

4.4 Eco Audit Modelling Sequence

The study uses level 3 Sustainability to identify significant environmental impacts in specific life cycle phases of high-pressure turbine blades used in commercial flights for short haul distance, covering the entire life cycle the subsections are arranged based on the tool's modelling sequence.

4.4.1 The material, manufacturing, and end of life phases

For this phase, we considered the turbine blades that will be placed in the initial section of the engine. We assumed 100 units for a batch with a blade mass of 2.3 kg for each turbine blade and the primary process being casting, as IN-738LC offers recyclability at the end of life, so recycling was selected with 30% as described above in the section 4.3.4

Material, manufacture and end of life

Components

Qty.	Component name	Material	Recycled content	Mass (kg)	Primary process	Secondary process	% removed	End of life	% recovered
100	High Pressure Turbine Blac	Nickel-Cr-Co alloy, IN-...	Virgin (0%)	2,3	Casting		0	Recycle	30

Figure 36. Material, manufacture and end of life particulars

4.4.2 Transport Phase

The short-haul air freight was recommended at a distance of 400 km, as a high distance would likely dominate energy usage and carbon emissions. The aim was to determine if other phases were dominant at this distance, below 500 km.

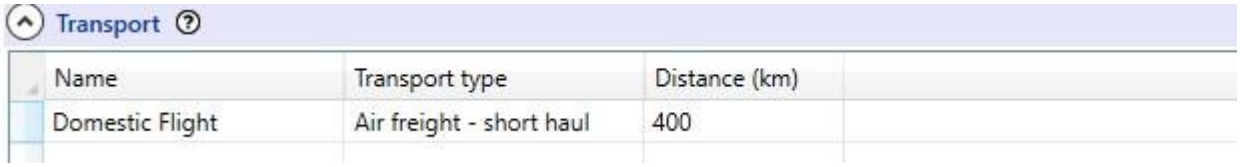

Figure 37. Transport phase particulars

4.4.3 The Use phase

We assumed that the average product life of a turbine blade subjected to high pressure was 10 years, supported by the fact that, in the worst-case scenario, if the turbine blade begins to fail, which can be improved during the first fifth year of maintenance, it may need to be replaced at the end of 10 years. Kerosene was chosen as the fuel. We assumed utilization for 300 days, with 1600 km of travel every day and four trips.

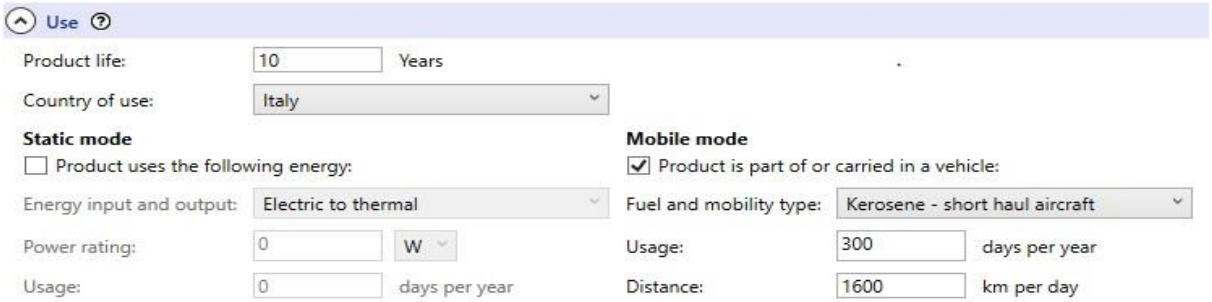

Figure 38. The Use Phase particulars

4.5 Assessments of the Eco-audit Reports

The Granta Software report indicates that the use phase is responsible for the majority of energy consumption and carbon emission as shown in the figure .39 below, which can be estimated by multiplying this by product weight and distance carried. The use phase consumes 99.1% of energy, consuming 14,400 thousand MJ, while the total energy consumed for the first life is 14,500 MJ thousands. Additionally, 99.4% of CO2 emissions are generated by the use phase, generating 1,030 thousand kg of CO2 footprint as shown in table. 2 below.

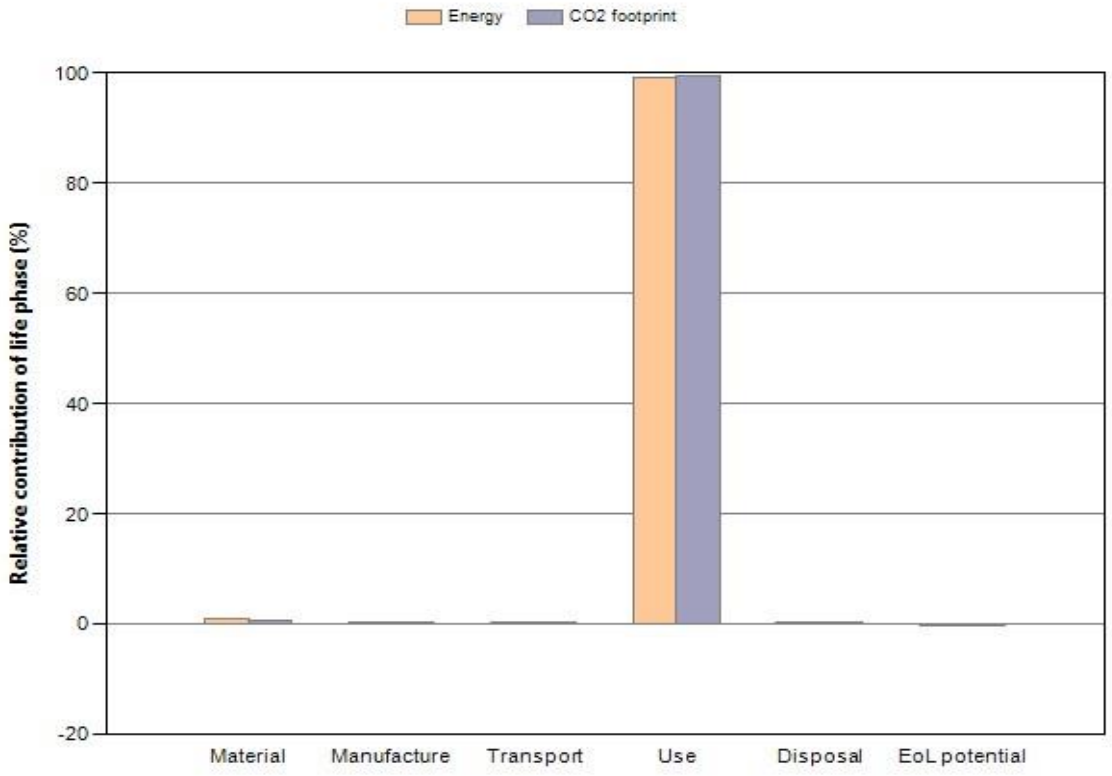

Figure 39. Th energy and carbon footprint breakdown for high pressure turbine blade in %

Table 2. The energy and carbon footprint breakdown for high pressure turbine blade by value

Phase	Energy (MJ)	Energy (%)	CO2 footprint (kg)	CO2 footprint (%)
Material	1,2e+05	0,8	5,85e+03	0,6
Manufacture	2,43e+03	0,0	182	0,0
Transport	1,2e+03	0,0	86,1	0,0
Use	1,44e+07	99,1	1,03e+06	99,4
Disposal	80,5	0,0	5,64	0,0
Total (for first life)	**1,45e+07**	**100**	**1,04e+06**	**100**
End of life potential	-3,23e+04		-1,48e+03	

The strategies for reducing environmental impact depend on the product type and dominant static or mobile use phase. For our application, mobile phase is dominant, Prioritizing mass reduction in component design directly addresses the dominant phase observed in eco-audits [16]. lean design involves using minimal material, but minimizing mass may not minimize embodied energy or cost [16]. Trade-off methods are used to resolve this conflict. Our efforts to reduce environmental effects and preserve energy are linked with our mass reduction goal.

5 Conclusion

This material and design project focused on material selection processes through Granta Edupack software for first stage HP turbine blade of a Turbofan engine. The primary aim was to determine materials that can withstand high service temperature, high pressure and centrifugal load of turbine blade which has properties of excellent creep strength, maximum fatigue strength, maximum fracture toughness and minimum weight.

The range of possible materials was quickly reduced from more than 4000 materials by screening using a Limit stage selection by restricting the choices to those materials that met the processability criteria or constraints. Depending on the thermal, mechanical and durability constraints, around **178** materials remain for ranking. Using Granta EduPack, it is easy to graphically display the objectives and remaining materials to analyze the trade-off between the performance indices.

The Performance index which a formula describing the combination of material properties that must be minimized or maximized to make an optimal choice for a particular design objective by taking an assumption of uniform loading at cantilever beam with constant aspect ratio. Finaly **8** candidate materials were extracted after applying minimized mass, maximize fracture toughness and maximize fatigue strength of performance index. Among those candidate material, **Nickel Cr-Co alloy IN-738LC** was chosen depending on its castable properties and commonly applicable in turbine blade material due to Edupack database. Inconel 738LC has an exceptional creep resistance property due to the formation of fine, dispersed particles called gamma prime (γ') precipitates.

In the context of sustainability, the use phase is the main contributor to energy consumption and CO2 emissions, accounting for 99.1% and 99.4%, respectively. To minimize environmental impact, component design strategies must focus on mass reduction, while lean design aims for minimal material use, but this may not necessarily reduce energy or cost. Trade-off methods must be used to resolve this conflict.

6 References

[1] M. Yadav, A. Misra, A. Malhotra, and N. Kumar, "Design and analysis of a high-pressure turbine blade in a jet engine using advanced materials," *Mater. Today Proc.*, vol. 25, pp. 639–645, 2019, doi: 10.1016/j.matpr.2019.07.530.

[2] T. O. F. Contents, "gas-turbine engine".

[3] A. Ikpe, O. EFE-ONONEME, and G. ARİAVİE, "Thermo-Structural Analysis of First Stage Gas Turbine Rotor Blade Materials for Optimum Service Performance," *Int. J. Eng. Appl. Sci.*, vol. 10, no. 2, pp. 118–130, 2018, doi: 10.24107/ijeas.447650.

[4] M. F. Ashby and C. A. Abel, "Materials selection to resist creep," *Philos. Trans. R. Soc. A Math. Phys. Eng. Sci.*, vol. 351, no. 1697, pp. 451–468, 1995, doi: 10.1098/rsta.1995.0046.

[5] J. Kumar Singh Jadon, R. Singh, and J. Kumar Mahato, "Creep-fatigue interaction behavior of high temperature alloys: A review," *Mater. Today Proc.*, vol. 62, pp. 5351– 5357, 2022, doi: 10.1016/j.matpr.2022.03.487.

[6] G. J. Tatlock, T. J. Hurd, and J. S. Punni, "High Temperature Degradation of Nickel Based Alloys.," *Platin. Met. Rev.*, vol. 31, no. 1, pp. 26–31, 1987, doi: 10.1595/003214087x3112631.

[7] C. Dahal, J. K. Tharu, and H. B. Dura, "Thermo-Structural Analysis of High-Pressure Turbine Blade," vol. 15, no. 3, pp. 78–82, 2019.

[8] I. Aniekan Essienubong, O. Ikechukwu, P. O. Ebunilo, and E. Ikpe, "Material Selection for High Pressure (HP) Turbine Blade of Conventional Turbojet Engines," *Am. J. Mech. Ind. Eng.*, vol. 1, no. 1, pp. 1–9, 2016, doi: 10.11648/j.ajmie.20160101.11.

[9] B. A. Mohamad and A. Abdelhussien, "Failure analysis of gas turbine blade using finite element analysis," *Int. J. Mech. Eng. Technol.*, vol. 7, no. 3, pp. 299–305, 2016.

[10] M. Ashby, H. Shercliff, and D. Cebon, "B5796512C35F04C0E84a3Fb95388Ce4Aa000".

[11] S. M. Arnold, D. Cebon, and M. Ashby, "Materials selection for aerospace," *Introd. to Aerosp. Mater.*, no. October, pp. 569–600, 2012, doi: 10.1533/9780857095152.569.

[12] Z. Wang, Y. Su, and J. Feng, "high pressure Turbine blades of conventional turbojet engines," vol. 2, no. 2, pp. 171–176.

[13] H. Liu, J. Sun, S. Lei, and S. Ning, "In-service aircraft engines turbine blades life prediction based on multi-modal operation and maintenance data," *Propuls. Power Res.*, vol. 10, no. 4, pp. 360–373, 2021, doi: 10.1016/j.jppr.2021.09.001.

[14] L. Sun, Y. Sun, Y. Liu, N. Dai, J. Li, and Y. Jiang, "Effect of annealing temperature on pitting behavior and microstructure evolution of hyper-duplex stainless steel 2707," *Mater. Corros.*, vol. 70, no. 9, pp. 1682–1692, 2019, doi: 10.1002/maco.201910801.

[15] Z. Mazur, G. D. Ortega-Quiroz, and R. García-Illescas, "Evaluation of creep damage in a gas turbine first stage blade," *Int. Conf. Nucl. Eng. Proceedings, ICONE*, vol. 1, no. August, pp. 531–536, 2012, doi: 10.1115/ICONE20-POWER2012-55087.

[16] K. T. Gradin and A. H. Åström, "Evaluation of an Eco Audit tool - through an LCA of a novel car disc brake," *Proc. Nord. Des. Era Digit. Nord. 2018*, 2018.

[17] M. Ashby, P. Coulter, N. Ball, and C. Bream, "Granta EduPack Eco Audit Tool-A White Paper," no. October, pp. 1–27, 2021.

[18] C. Ghenai, "Eco Audits and Selection Strategies for Eco Design," *Ninth LACCEI Lat. Am. Caribb. Conf. (LACCEI'2011), Eng. a Smart Planet, Innov. Inf. Technol. Comput. Tools Sustain. Dev.*, no. August, pp. 1–11, 2011.

[19] D. Cebon, M. F. Ashby, C. Bream, and L. Lee-Shothaman, "CES EduPack User's Manual, Release 4," 2009, [Online]. Available: http://www.grantadesign.com/download/pdf/EduPack-2009-Manual.pdf

[20] E. C. Milan Grohol, Constantze Veeh, DG GROW, *Study on the critical raw materials for the EU 2023*, vol. 6, no. 1. 2017. [Online]. Available: http://repositorio.unan.edu.ni/2986/1/5624.pdf%0Ahttp://fiskal.kemenkeu.go.id/ejournal%0Ahttp://dx.doi.org/10.1016/j.cirp.2016.06.001%0Ahttp://dx.doi.org/10.1016/j.powtec.2016.12.055%0Ahttps://doi.org/10.1016/j.ijfatigue.2019.02.006%0Ahttps://doi.org/10.1

[21] H. Wang *et al.*, "Selective laser melting of the hard-to-weld IN738LC superalloy: Efforts to mitigate defects and the resultant microstructural and mechanical properties," *J. Alloys Compd.*, vol. 807, 2019, doi: 10.1016/j.jallcom.2019.151662.

[22] M. L. Grilli *et al.*, "Critical raw materials saving by protective coatings under extreme conditions: A review of last trends in alloys and coatings for aerospace engine applications," *Materials (Basel).*, vol. 14, no. 7, 2021, doi: 10.3390/ma14071656.

[23] G. Genchi, A. Carocci, G. Lauria, and M. S. Sinicropi, “Ijerph-17-00679-V3.Pdf,” *Int. J. Environ. Res. Public Health*, vol. 17, no. 3, pp. 679–700, 2020.

[24]https://www.researchgate.net/profile/Lakshya_Kumar_A/publication/334737601/figure/download/fig1/AS:785956336590848@1564398001505/Cross-section-of-a-turbofan-engine-1.ppm]

[25]https://www.researchgate.net/profile/Kyung_Choi2/publication/223630713/figure/fig5/AS:523496401969154@1501822676654/Turbine-blade-physical-model.png.

[26] https://eaglepubs.erau.edu/introductiontoaerospaceflightvehicles/chapter/turbojet-engines/

[27] Thermal shock resistance of materials (thermal-engineering.org)